Simulation of an Axial Vircator

V. V. Tikhomirov*, S.E. Siahlo

September 26, 2013

Research Institute for Nuclear Problems, Belarusian State University,
Bobruiskaya 11, 220030 Minsk, Belarus

Abstract

An algorithm of particle-in-cell simulations is described and tested to aid further the actual design of simple vircators working on axially symmetric modes. The methods of correction of the numerical solution, have been chosen and jointly tested, allow the stable simulation of the fast nonlinear multiflow dynamics of virtual cathode formation and evolution, as well as the fields generated by the virtual cathode. The selected combination of the correction methods can be straightforwardly generalized to the case of axially non-symmetric modes, while the parameters of these correction methods can be widely used to improve an agreement between the simulation predictions and the experimental data.

1 Introduction

The advancements in the development of high power microwave (HPM) pulsed power sources greatly contribute to the progress in many branches of science and technology. Their most important applications are pulsed heating of plasma, acceleration of high-current electron or ion beams, feeding of high-power radar systems, pumping of high-power excimer lasers, destruction of atmospheric freon to protect the ozone layer. They are hoped to find applications in the equipment vulnerability testing as well as in the development of defense systems.

Vircators, based on the oscillations of a dense electron bunch, called the virtual cathode (VC), – are believed to be promising microwave pulsed power sources with the output power up to 10 GW and more [1, 2]. They have many advantages over more conventional devices, including the simplicity of the hardware design, compactness, the ability to operate in the absence of an external magnetic field, the potential for tuning frequency, moderate requirements to the beam's quality and the simple waveguide configuration. What is more, they can serve as pulsed sources of electrons and neutrons. Unfortunately, currently available vircators have not very high efficiency and unstable generation frequency.

The use of electron beams with currents exceeding the space-charge limiting current represents the principle virtue of vircators. Moving downstream of the anode along of the waveguide, an electron beam is slowed-down and forms a VC. The growing electric field of the VC reflects the newly incoming electrons, forcing them to oscillate between the virtual and real cathodes. Reflection, mutual repulsion, and the electron drift beyond the VC cause it to destruct. The accompanying VC charge and shape oscillations, together with the electron oscillations are the sources of intense radiation.

*E-mail:vvtikh@mail.ru

That the electrons motion is strongly nonlinear, unsteady, and multi-flow allows one to study and design vircators only proceeding from the first principles of electrodynamics and kinetics that are conventionally implemented in the particle-in-cell (PIC) method that combines the finite-difference formulation of Maxwell's equations and finite-size particle method [3, 4]. Having no alternative for solving a wide range of problems dealing with the application of supercritical currents, this approach has been implemented in a range of computer codes, such as MAGIC [5] and KARAT [6]. It is essential that the discrete methods of the solution of Maxwell's equations cannot be used without regular corrections and smoothing (numerical filtering) of numerical solutions for the fields, as well as charge and current densities. The methods and techniques for these correction procedures vary greatly and sometimes lack a serious ground. This limits the possibility to check and adjust such procedures within the standard codes. However, holding complete information about the correction and smoothing procedures, the developer has every possibility to optimize these procedures and adjust them to specific applications, as well as to involve experimental data in the code. This point demonstrates the obvious need for self-developed simple codes based on the particle-in-cell method for the solution of Maxwell's equations. This paper presents the first version of our self-developed code enabling an adequate simulation of the nonstationary, nonlinear dynamics of supercritical electron beams in the gigawatt-range axial vircators of the simplest configuration that operate on axially-symmetric modes.

2 Numerical Solution Algorithm

2.1 Finite-difference Scheme and Boundary Conditions

Let us recall briefly the general approach to the solution of Maxwell's equations by the particle-in-cell method [3–6] by giving specific examples of the applied procedures. Conventionally, electric and magnetic fields are divided into quasi-static external fields and rapidly changing "internal" ones that are induced by the charges and currents of the system. The quasi-stationary accelerating field is determined by the potential of the electrodes and can be found by solving Laplace's equation, while the internal fields are determined by the boundary conditions and are obtained from Maxwell's equations. Following [5,6], we shall solve Maxwell's equations using the leapfrog method and the Yee mesh comprised of simple rectangular grids (or meshes) shifted in space and time, confining ourselves to the consideration of quite simple constructions [1, 2, 6–8] with circular waveguides, efficiently operating on axially symmetric modes TM_{0i} (note that for coaxial vircators it is crucial that axially assymmetric modes be taken into account). Our system is described by the following finite-difference scheme:

$$
\begin{aligned}
&\frac{(E_r)^{n+1}_{i-1/2,k} - (E_r)^{n}_{i-1/2,k}}{c^2\tau} = \\
&-\frac{(B_\theta)^{n+1/2}_{i-1/2,k+1/2} - (B_\theta)^{n+1/2}_{i-1/2,k-1/2}}{h_z} - \mu_0 \left(J_r\right)^{n+1/2}_{i-1/2,k}, \\
&\frac{(E_z)^{n+1}_{i,k-1/2} - (E_z)^{n}_{i,k-1/2}}{c^2\tau} = \\
&\frac{r_{i+1/2}\left(B_\theta\right)^{n+1/2}_{i+1/2,k-1/2} - r_{i-1/2}\left(B_\theta\right)^{n+1/2}_{i-1/2,k-1/2}}{r_i h_r} - \mu_0 \left(J_z\right)^{n+1/2}_{i,k-1/2}, \\
&\frac{(B_\theta)^{n+1/2}_{i-1/2,k-1/2} - (B_\theta)^{n-1/2}_{i-1/2,k-1/2}}{\tau} = \\
&\frac{(E_z)^{n}_{i,k-1/2} - (E_z)^{n}_{i-1,k-1/2}}{h_r} - \frac{(E_r)^{n}_{i-1/2,k} - (E_r)^{n}_{i-1/2,k-1}}{h_z}.
\end{aligned}
\tag{1}
$$

In these equations E_r and E_z are the radial and longitudinal components of the electric field, B_θ is the azimuthal component of the magnetic field, and J_r and J_z are the radial and longitudinal components of the current density, respectively. The indices i and k in Eqs.(1) correspond to the numbers of the grid points (or grid nodes) along the $0r$ and $0z$ axes, whose coordinates are $r_i = (i-1)h_r$ and $z_k = (k-1)h_z$, where h_r and h_z are the radial and longitudinal dimensions of the cells in the $(r-z)$ plane, respectively; τ is the time step, and n is the step number. The quantities $n \pm 1/2, i-1/2$, and $k-1/2$ correspond to the intermediate time moments $(n \pm 1/2)\tau$ and "half-cell" coordinates $r = (i-3/2)h_r$ and $z = (k-3/2)h_z$, respectively. The time and coordinate steps satisfy the Courant stability condition

$$c\tau < \sqrt{h_r^2 + h_z^2}\ . \tag{2}$$

The vircators considered here are simple in design: they consist of a tubular section and meandres with rectangular cross sections by rz plane [7, 8] (Fig.1); metal surfaces are parallel to either the $0r$-axis (the emitting surface of the cathode, anode mesh, and frontal surfaces of the meandres) or the $0z$-axes (outer walls of the diode, the cathode-holder, the resonator and the faces of the meandres). The condition of perfect conductivity for these two types of surfaces takes the forms $E_r = 0$ and $E_z = 0$, respectively.

The emitted-wave output from the resonator is provided by the condition

$$c\frac{(B_\varphi)^{n+1/2}_{i-1/2,k+1/2} + (B_\varphi)^{n-1/2}_{i-1/2,k-1/2}}{2} = (E_r)^n_{i-1/2,k} \tag{3}$$

for the longitudinal index $k = z_{ex}/h_z + 1$ corresponding to the coordinate z_{ex} of the output window. The output power of the vircator is calculated by integrating the Poynting vector $S = E_r H_\phi$ over the output window area.

The finite-difference equations (1) imply that the current densities J_r and J_z are specified in discrete "half-cell" locations of the grid: $(i-3/2)h_r$, $(k-1)h_z$ and $(i-1)h_r$, $(k-3/2)h_z$, respectively. At the same time, the particle motion defined by the sum of external and internal fields is continuous and can be described by the Newton-Lorentz equation that includes the electric and magnetic fields strengths at continuously distributed points.

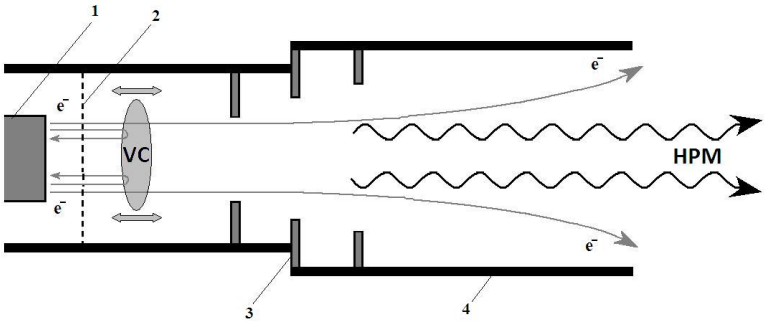

Figure 1: Central longitudinal cross section of the axial vircator: 1 - cathode, 2 - anode mesh, 3 - meander of the resonator, 4 - side wall of the resonator. Oscillations of the virtual cathode (VC) together with the oscillations of electrons between the VC and the real cathode, are the sources of high-power microwave (HPM) radiation.

A key to the successful implementation of the PIC method is the proper direct and inverse conversion between the physical quantities defined in a continuous space and on the discrete

grid [3,4]. In the PIC method, there is a constant interplay between the grid and the particles as the grid quantities are used to define forces which move the particles, and the particles "send" position and velocity information back to the grid. The conversion between the continuous space and the grid is performed using weight functions that depend on the distance between the particle position and the coordinate of the grid point.

We have verified the adequate efficiency of the first-order weighting (also called area weighting) [3,4], implying that the point charge located at the continuous particle position is allocated to the grid points surrounding the particle by the linear interpolation formulas. At each time step the weighting procedure is employed twice. First for the interpolation of continuous charge and current densities to discrete grid points for solving the Poisson (see in what follows) and Maxwell's equations, and second for the interpolation of the fields, found from Maxwell's equations in the grid points, to continuously distributed particles. To achieve a sufficient accuracy of the procedure repeated at each time step, it is essential that the same weight function be used for both direct and inverse interpolations [3, 4]. It now remains to add that the fields interpolated to continuously distributed points are applied to find particle trajectories by solving the Newton-Lorentz equation written in a time-centered form and solved using the algorithm suggested by Boris (see [3]).

2.2 Correction of the numerical solution

Note should be taken of the fact that the simulation of electron distribution in a phase space by macro (finite-size) particles, each containing more than 10^9 electrons, is a radical step, and one who takes it should be perfectly aware and capable of overcoming consequences. The problem is that the number of macro particles in a spatial cell is always relatively small, which makes the continuity limit unachievable even with the maximal computational power. For this reason, the components of the current density on the right-hand sides of Ampere's law in Eq.(1) are a permanent powerful source of numerical noise on the scale defined by the cell size of the spatial grid. Though the processes of interest for simulation (first and foremost, formation and evolution of a virtual cathode and the related induced fields) manifest themselves over longer spatial scales, the presence of a permanent powerful source of high-frequency noise inevitably affects the behavior of macro particles, eventually causing nonphysical oscillations at intermediate frequencies. This particle-induced noise precludes the adequate description of the beam behavior on the most relevant space-time scales and contaminates the physics of interest [3–6].

The reduction of this high-frequency noise through filtering the fields enables one not only to obtain comprehensive results with a limited number of macro particles in a cell with long-available computational powers, but even to pass beyond the Courant stability conditions (2) [5]. Though justified from the physical viewpoint, filtering is a kind of an artificial trick, and so it is pointless, or at least premature to discuss the optimal procedures for it. After years of research, the simulation community actually has developed original approaches to the implementation of filtering, whose correctness and efficiency were confirmed by the experimental results [3–6]. Based on their experience and governed by the objectives of our team, we use here the filtering procedure that seems simple, reliable, and beneficial in developing high-power axial vircators.

Historically, the first problem recognized and solved was the violation of the Gauss law $\nabla \cdot \mathbf{E} = \rho/\varepsilon_0$, equivalent to the charge conservation equation $\nabla \cdot \mathbf{J} + \partial\rho/\partial t = 0$ violation. The most popular and effective method for eliminating this problem is the Boris correction procedure [3]: finding the correction potential Φ that satisfies the Poisson equation $\Delta\Phi = \nabla \cdot \mathbf{E} - \rho/\varepsilon_0$ and replacing the field $\mathbf{E}$ by $\mathbf{E} - \nabla\Phi$. Though the approach is always basically the same, the procedures may vary. For example, the simultaneous over relaxation method for integrating Poisson's equation that is used in the code "KARAT" [6], is completed for better convergence by

the embedded grid method with Chebyshev acceleration. The adoption of such a highly accurate approach in this context seems redundant, and this is not only because of possible considerable increase of computational time. What really seems redundant is a too high accuracy when finding solutions that give mainly nonphysical information about the current density numerical noise due the use of the PIC method. These considerations have led us to the application of a much more simple, fast, but adequate procedure: use the minimal number of iterations of the Jacobi (or point Jacobi) iterative method, the simplest of all iterative methods. One might argue that the Jacobi method has a slow convergence, requiring hundreds and more iterations. However, tens of thousands of iterations are performed while integrating Eq. (1) over time, and so a single pass of Jacobi iteration at each time step suffices to keep the high-frequency noise, induced by the PIC method, on the level preventing nonphysical phenomena on the VC characteristic space-time scale. A similar grounding can well be applied to the Marder's correction algorithm [9]. Our approach can be considered as a more demonstrative and simple, but a fully-functional analogue thereof [10].

Let us note that the simplicity of this approach enables a significant number of iterations of Poisson's equation for the correction potential Φ at each time step without a noticeable slowing down of the entire simulation procedure. Usually, the number of iterations can be as large as tens, while for small spatial areas, such as the accelerating gap between the cathode and the anode, this number can even reach hundreds. In such correction procedure the increasing number of iterations leads to some reduction in the radiation power and a smother distribution of the fields. This suggests that the numbers of iterations in different parts of the vircator construction can also be used as the model parameter to improve the agreement with experimental or some other simulation data.

The correction of the current density instead of a longitudinal component of the electric field [5] can also compensate for the deviation from Gauss's law. At any rate, the correction procedure involves the quantities specified at the same time moment and is a centered-difference and time-reversible procedure [3]. Along with electrostatic fluctuations, the errors in the current density interpolation lead to the excitation of the transverse electric fields, whose amplitudes grow in time in the absence of attenuation, thus making increased contributions to the rotors of the electric and magnetic fields in Eq. (1). Earlier for the suppression of short-wave transverse fields, the simplest filtering procedure was used, which means averaging of the filtered quantities over the neighboring grid points with commonly used weights [3,4,6]. At present, a time-biased (or time-uncentered) semi-implicit scheme due to B. Godfrey [11] is more widely used for filtering particle noise. This procedure implies that I number of iterations ($i = 1...I$) of the Ampere and the Faraday equations are performed at each time step and in each point of the grid

$$\begin{aligned} E^{n+1,i} &= (1-\tau_i)\, E^{n+1,i-1} + \tau_i E^{n,I} \\ &+ \tau_i \delta t \left[-J^{n+1/2}/\varepsilon_0 + \nabla \times \left(a B^{n+3/2,i-1} + (1-a)\, B^{n+1/2,I} \right) / \left(\mu_0\, \varepsilon_0 \right) \right], \\ B^{n+3/2,\,i} &= B^{n+1/2,I} - \delta t\, \nabla \times E^{n+1,\,i}. \end{aligned} \tag{4}$$

These iterations result in a selective suppression of the field amplitudes in the upper spectral range; the degree of such filtering, as well as the essential number of iterations, I, grows as the parameter a increases from zero to unity. To provide an optimal degree of spectral filtering, the following expression for the iteration coefficients is used [5]:

$$\tau_i = \left\{ 1 + 2\, a \left\{ 1 - cos\left[\pi \left(i - 1/2 \right) / I \right] / cos\left(\pi / \left(2I \right) \right) \right\} / \left(1 - a \right)^2 \right\}^{-1}. \tag{5}$$

Now, the parameters a and I for the correction of a transverse field are selected by experience. When the stability of the integration scheme is ensured, these parameters can be further adjusted to achieve a better agreement with the experiment.

2.3 Injection of current restricted by space charge

As is well known [12, 13], the supercritical currents are generated through explosive electron emission. The magnitude of the current density J_z injected from the cathode is limited by the density of a space charge, whose presence leads to vanishing of the normal component of the electric field on the emitting surface. The tangential component J_r there naturally goes to zero too. Under such conditions Gauss's theorem for the i-th grid cell with $0 < z < h_z/2$ and $0 < r < h_r/2$ at $i = 1$, and $h_r\,(i - 3/2) < r < h_r\,(i - 1/2)$ at $i = 2, 3, \ldots$ allows one to define the charge values

$$\Delta Q_i = \pi\varepsilon_0 h_r \left\{ \frac{1}{4} h_z \left[\left(i - \frac{1}{2} \right) (E_r)_{i-1/2,2} - \left(i - \frac{3}{2} \right) (E_r)_{i-3/2,2} \right] + (i-1)\, h_r\, (E_z)_{i,1} \right\} - Q_i, \quad i = 2, 3, \ldots$$

$$\Delta Q_1 = \pi\varepsilon_0 h_r \left\{ \frac{1}{8} h_z\, (E_r)_{1/2,2} + \frac{1}{4} h_r\, (E_z)_{1,1} \right\} - Q_1, \tag{6}$$

to be injected into these cells to fulfill Gauss's low at the current time step. The problem of charges ΔQ_i location inside the cells does not have an unambiguous solution. Quasi-uniform charge emission near the cathode surface seems to be quite natural at first glance.

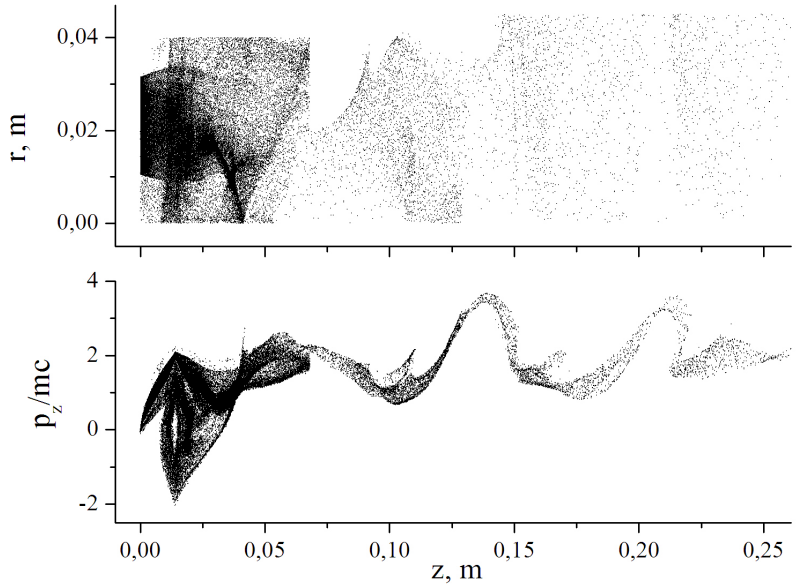

Figure 2: Configurational (top) and longitudinal phase portrait of the beam in the axial vircator.

However linear extrapolation of the electric field does not provide adequate values of the accelerating field near the cathode. The small field magnitudes resulting from the vanishing normal component of the field near the cathode surface, lead to the excessive influence of the field interpolation inaccuracy on the slow particle motion near the cathode surface. Being thus unable to rigorously define the spatial distribution of the injected electrons, the authors of [14] suggested that the emitted electrons be placed at the centers $r_i = h_r(i-1)$, $i = 1, 2\ldots$, $z = h_z/4$ of the cells that are contiguous with the cathode surface. Our proposal is also to inject electrons in the plane $z = h_z/4$, however to distribute them quasiuniformly over r^2.

3 Example of Axial Vircator Simulation

By way of example, we shall consider the axial vircator simulated and tested in [8]. According to Eqs. (1), under the conditions of axial symmetry, the electron density oscillations produce spatially and temporally varying longitudinal and radial currents. These currents induce the corresponding components of the electric field both of which in turn induce the azimuthal magnetic field. Under vanishing tangential components of the electric field on the walls of a closed cylindrical resonator of radius R and length L TM_{0il} resonator modes

$$\begin{aligned} E_z &= E_0 J_0(k_\perp r)\cos k_z z, \\ E_r &= E_0 \frac{k_z}{k_\perp} J_1(k_\perp r)\sin k_z z, \\ B_\varphi &= iE_0 \frac{\omega}{k_\perp c^2} J_1(k_\perp r)\cos k_z z \end{aligned} \tag{7}$$

will be generated, where $k_\perp = \lambda_i/R$, λ_i are the roots of zero-order Bessel function, $J_0(\lambda_i) = 0$; $k_z = \pi l/L$, $l = 1, 2, ...$, $\omega = c\sqrt{k_z^2 + k_\perp^2}$ is the frequency, and E_0 is the amplitude of the wave.

But to provide the radiation output, the passage is required between the resonator and the diaphragmatic waveguide that must be constructed to provide both the effective resonance interaction of radiation and VC in the resonator and the radiation output from the latter. It follows from the above that the standing waves (7) transform into traveling waves TM_{0i} with the same radial distribution of the intensities.

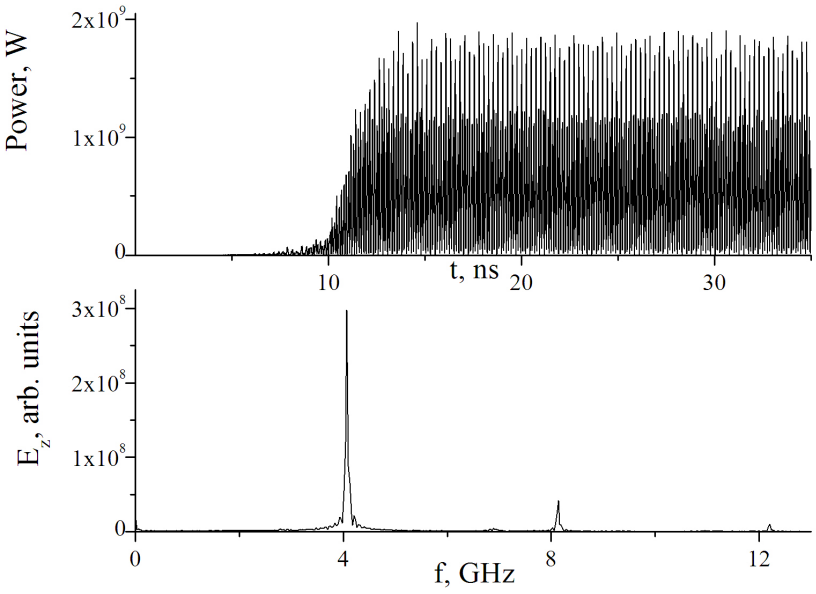

Figure 3: Power vs time (top) and the radiation spectrum (bottom) of the axial vircator.

The generation frequency $f = 4-4,1$ GHz and the radius $R = 4$ cm of the resonator section of the waveguide enable choosing the section length $L = 5,4$ cm to provide the predominate generation of the lowest TM_{011} mode. The dimensions of the other sections of the waveguide, pictured in Figs. 1 and 3 [8], were reconstructed by E.A.Gurnevich; following [8], the outer and inner radii of the annular cathode and the cathode-anode gap were taken equal to 32, 12, and 14 mm, respectively, and the mesh transparency was taken as 70%. The simulation results for the cathode-anode voltage of 630 kV are given in Figs. 2 and 3. Electron distribution in the

configurational and the longitudinal phase space (Fig.2) illustrate the main features of the VC dynamics, as well as the significant pulse modulation of the electrons propagating behind the VC. As is seen, the average radiated power is close to 1 GW and the generation frequency, to 4.1 GHz (see Fig. 3), as reported in [8].

Let us note that the electrons behind the VC are sometimes accelerated to the energies exceeding by a factor of two and more the acceleration energy in the cathode-anode gap, and also have a rather large energy when they leave the resonator (compare with [7]). One can guess that the radiation generated by vircator can be increased by removing the electrons from the acceleration process in the resonator in the regions, where their energy is minimal, e.g. using local external fields.

4 Conclusion

An algorithm of particle-in-cell simulations was described and tested to aid further the actual design of simple vircators working on axially symmetric modes. The methods of correction of the numerical solution, which were selected and jointly tested, allow the stable simulation of the fast nonlinear multiflow dynamics of the virtual cathode emergence and evolution, as well as the fields generated by the virtual cathode. The chosen combination of correction methods can be straightforwardly generalized to the case of axially nonsymmetric modes, while the correction methods parameters can be widely used to improve an agreement between the simulation predictions and the experimental data.

5 Acknowledgements

The authors are grateful to Vladimir Baryshevsky for suggesting the research topic. The authors also wish to acknowledge the cooperation and useful discussions with and V.G. Baryshevsky, A.A. Kuraev, S.V. Anishchenko, A.A. Gurinovich, E.A.Gurnevich, P.V. Molchanov, and S.N. Sytova.

References

[1] Rukhadze A.A., Stolbetsov S.D. and Tarakanov V.P., *Radiotekh.Elektron.* (Moscow),1992, Vol. 37, N 3, P. 385;

[2] Dubinov A.E., Selemir V.D. *Radiotekh.Elektron.* (Moscow), 2002, Vol. 47, P.645-672 [*J. Commun. Technol. Electron.* 2002, Vol. 47, P.645];

[3] Birdsall C.K., Langdon A.B. Plasma Physics via Computer Simulation. New York:McGraw-Hill, 1991;

[4] Hockney R.W, Eastwood J.W. Computer simulation using particles. New York:McGraw-Hill, 1981, P. 640;

[5] Goplen B., Ludeking L, Smithe D., Warren G. *Comp .Phys. Comm.* 1995, Vol. 87, P. 54-86;

[6] Tarakanov V.P., 'User's Manual for Code KARAT', BRA Inc., Va, USA. 1992;

[7] Altercorp B.A., Rukhadze A.A., Sokulin A.Yu. and Tarakanov V.P. *Zh. Tekh. Fiz.* 1991, Vol. 61, N 9, P. 115;

[8] Li Z.-Q., Zhong H.-H., Fan Y.-W., Shu T., Yang J.-H., Yuan C.-W., Xu L.-R., Zhao Y.-S. *Chin. Phys. Lett.* 2008, Vol. 25, N 7, P. 2566-2568;

[9] Marder B., A Method for incorporating Gauss' law into electromagnetic PIC codes, *J. Comput. Phys.* 68, N 1, (1987):

[10] Langdon A. B. *Comp .Phys. Comm.* 1992, Vol. 70, P. 447-450;

[11] Godfrey B.B. and Goplen B., Practical evaluation of time-biased electromagnetic field algorithms for plasma simulations, in 22 Annual meeting of APS, Division of plasma physics, 10-14 November, 1980 / Mission Res. Corp., Lancaster, PA, AMRC-N-146, Nov. 1980;

[12] Mesyats. G.A. Pulsed power and electronics. Moscow: Nauka, 2004. P.704;

[13] Miller R.B., Introduction to the physics of charged particle beams. New York:Plenum, 1982, P. 432;

[14] Watrous J.J., Lugisland J.W. and Sasser III G.E. *Phys. Plasm.* 2001. Vol. 8. N 1 PP. 289-296.